JOURNAL OF CATALYSIS 93, 459–466 (1985)

Catalytic Properties of $La_{1-x}A'_xFeO_3$ (A' = Sr,Ce) and $La_{1-x}Ce_xCoO_3$

TAIHEI NITADORI[1] AND MAKOTO MISONO[2]

Department of Synthetic Chemistry, Faculty of Engineering, The University of Tokyo, Bunkyo-ku, Tokyo, 113 Japan

Received July 11, 1984; revised November 29, 1984

The catalytic properties of perovskite-type mixed oxides ($LaFeO_3$ and $LaCoO_3$) have been investigated, with regard to the effects of Sr^{2+} and Ce^{4+} substitution for La^{3+}. In the case of $La_{1-x}Sr_xFeO_3$ (x = 0–0.6), the catalytic activities for propane oxidation increased with x when x was low, but decreased at higher x values. The capability of dissociating oxygen molecule (rate of isotopic equilibration) varied with x in parallel with the catalytic activity, while as in the case of $La_{1-x}Sr_xCoO_3$ the readiness of oxygen desorption increased monotonously with the Sr^{2+} content, x. Upon the Ce^{4+} substitution (x = 0.1), the readiness of oxygen desorption and the rate of isotopic exchange of oxygen decreased for $LaFeO_3$, but they increased for $LaCoO_3$. Correspondingly, the catalytic activities increased for the Co system and slightly for the Fe system. These results have been explained on the basis of the actual Ce^{4+}-substitution ratio and the valence of active site.

INTRODUCTION

Perovskite-type mixed oxides (ABO_3) have a well-defined structure, and it is possible to change the A- or B-site ion variously, without affecting the fundamental structure (*1*). Owing to this nature, the oxidation state of B-site ion and the number of oxygen vacancies can be controlled. Therefore, perovskite-type mixed oxides are suitable materials for the study of the relationships between the solid-state chemistry and catalytic action of metal oxides. Furthermore, perovskite-type mixed oxides are interesting materials in practical uses. It has been reported that for complete oxidation their activities are comparable with or greater than that of Pt or Pd catalysts (*2–4*).

We previously reported that $La_{1-x}Sr_xCoO_3$ catalysts showed high activities in the oxidation of hydrocarbons and carbon monoxide, $La_{0.8}Sr_{0.2}CoO_3$ being the most active (*4*). We also found that the desorption of lattice oxygen, or the formation of oxygen vacancies, became easier with increasing Sr^{2+} substitution (x) and this tendency made the lattice oxygens more reactive. The variation of catalytic activity was well explained on the basis of reduction–oxidation properties of catalysts (*5, 6*).

In the present work, we investigated the effects of Sr^{2+} substitution in $LaFeO_3$ and Ce^{4+} substitution in $LaCoO_3$ and $LaFeO_3$. We attempted to elucidate the relationship between the catalytic properties and the structure and composition of the perovskite-type catalyst, emphasizing the reactivities of oxygen both in the bulk and on the surface.

EXPERIMENTAL

Catalysts

$La_{1-x}Ce_xCoO_3$ was prepared from mixtures of metal acetates of each component (*4, 6*). First, mixed acetate solution was evaporated to dryness in a rotary evaporator (70–90°C) and then the solid obtained was first decomposed in air at 300°C for 3 h and then calcined in air at 850°C for 5 or 10 h in an electric furnace. $La_{1-x}A'_xFeO_3$ (A' =

[1] On leave from Japan Tobacco & Salt Public Corporation.

[2] To whom all correspondence should be addressed.

0021-9517/85 $3.00

Sr,Ce) was prepared from mixtures of metal nitrates (*4*). The precipitates which were obtained by the coprecipitation from mixed nitrate solutions by *n*-butyl amine were filtered. They were decomposed and calcined in a similar manner as above. Powder X-ray diffraction (XRD) patterns were recorded on powder X-ray diffractometer (Rigaku Denki, Rotaflex, RU-200) using Cu$K\alpha$ radiation. Surface area of the samples was measured by BET method (N_2 adsorption).

Apparatus

Conventional flow, pulse, and closed-circulation systems as described before (*4–6*) were used.

Procedure

(*1*) *Oxidation of propane.* The oxidation reaction of propane was carried out with the flow system. Prior to the reaction, the catalysts (300 mg) were treated in an O_2 stream for 1 h at 300°C. A gas mixture of propane (0.83%), O_2 (33.3%), and N_2 (balance) was used in flow experiments. The flow rate of the mixed gas was 60 ml · min^{-1}. Products were analyzed by a gas chromatograph (silica gel, 1 m, kept at 84°C).

(*2*) *Temperature-programmed desorption (TPD) of oxygen.* TPD of oxygen was carried out with a flow system using helium as a carrier gas. Prior to each run, the sample (1 g) was treated in an O_2 stream for 1 h at 300°C and then cooled to room temperature in the O_2 stream. Then, a helium stream was substituted for an O_2 stream at room temperature. Oxygen impurity in He was removed by a molecular sieve 5A trap kept at liquid-nitrogen temperature. Then, the temperature of the sample was raised at a constant rate of 20°C · min^{-1} in the He stream (30 ml · min^{-1}), and oxygen desorbed was detected by use of a quadrupole mass spectrometer (NEVA, NAG-531). In the first run of TPD for each sample, CO_2 and H_2O evolved in addition to O_2. But in the subsequent runs, neither CO_2 nor H_2O was detected above background level, and TPD curves were reproducible. Data of the second runs were adopted in this paper.

(*3*) *Isotopic exchange and equilibration of oxygen.* ^{18}O Exchange between O_2 in the gas phase and oxygen in perovskite (denoted as "exchange" in this paper) and isotopic equilibration of O_2 in the gas phase ("equilibration") were conducted in the closed-circulation system. Prior to the reaction, the sample (300 mg) was treated with pure circulating O_2 (100 Torr) at 300°C (with a trap kept at liquid-nitrogen temperature) and subsequently evacuated for 1 h at 300°C. O_2 enriched in ^{18}O (70–75 at.%) was prepared by mixing $^{18}O_2$ (99.5%) purchased from Japan Radioisotope Association and pure $^{16}O_2$. ^{18}O distribution in O_2 in the gas phase was analyzed by a mass spectrometer (Hitachi Co. Ltd., RMU-S) after intermittent sampling.

RESULTS

Structure and Surface Area of the Catalysts

The surface area and the crystal structure of the prepared catalysts are summarized in Table 1. Perovskite-type structure of the samples was confirmed with reference to ASTM cards. In the range $0 \leqq x \leqq 0.2$, $La_{1-x}Sr_xFeO_3$ had the pure perovskite-type structure. (In this paper $La_{1-x}Sr_xFeO_3$ will be used as a general formula for $La_{1-x}Sr_xFeO_{3-\delta}$ ($\delta \geqq 0$), unless otherwise stated.) In the range $0.4 \leqq x \leqq 0.6$, $La_{1-x}Sr_xFeO_3$ with the perovskyte-type structure was the main phase, with a small portion of tetragonal $SrFeO_{3-\delta}$ as in the literature (*7*). In the case of $La_{1-x}Ce_xCoO_3$ and $La_{1-x}Ce_xFeO_3$, CeO_2 phase appeared. At the same x, XRD peaks of CeO_2 phase were greater in the Co system than in the Fe system; for example, CeO_2 phase was almost absent in $La_{0.9}Ce_{0.1}FeO_3$, while distinct CeO_2 peaks were observed in $La_{0.9}Ce_{0.1}CoO_3$ (Fig. 1).

Oxidation of Propane

Figure 2 shows the relative oxidation rate

TABLE 1

Surface Area and Structure of Catalysts

Catalyst	Calcination		Surface area ($m^2\ g^{-1}$)	Structure
	Temp., °C	Time, h		
$LaFeO_3$	850	5	6.8	P[a]
$La_{0.9}Sr_{0.1}FeO_3$	850	10	4.3	P
$La_{0.8}Sr_{0.2}FeO_3$	850	10	7.0	P
$La_{0.6}Sr_{0.4}FeO_3$	850	10	7.2	P + $SrFeO_{3-\delta}$
$La_{0.4}Sr_{0.6}FeO_3$	850	10	6.3	P + $SrFeO_{3-\delta}$
$La_{0.9}Ce_{0.1}FeO_3$	850	5	4.9	P + (CeO_2)
$La_{0.8}Ce_{0.2}FeO_3$	850	5	4.4	P + CeO_2
$LaCoO_3$	850	5	1.9	P
$La_{0.9}Ce_{0.1}CoO_3$	850	5	1.8	P + CeO_2
$La_{0.8}Ce_{0.2}CoO_3$	850	5	3.3	P + CeO_2

[a] Perovskite structure.

of propane at 227°C over $La_{1-x}Sr_xFeO_3$ ($0 \leqq x \leqq 0.6$) and $La_{1-x}Ce_xFeO_3$ ($0 \leqq x \leqq 0.2$) normalized to unit surface area. It is noted in this figure that in the case of Sr^{2+} substitution the oxidation activities of both x = 0.1 and 0.2 were about four times greater than that of x =0. This trend is similar to the $La_{1-x}Sr_xCoO_3$ system (*4–6*). In the case of the Co systems the activity for propane oxidation increased almost 10 times by the introduction of a small amount of Sr^{2+} (x = 0.1–0.2) (*4*). When Sr^{2+} substitution was more than x = 0.4, the catalytic activity decreased significantly both for Co and Fe systems. In the case of Ce^{4+} substitution, the catalytic activity of both Co and Fe systems increased at x = 0.1, but it decreased at x = 0.2 (Figs. 2 and 3).

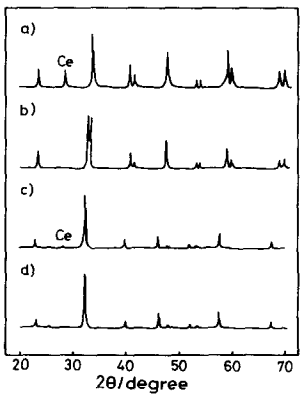

FIG. 1. XRD patterns of catalysts. (a) $La_{0.9}Ce_{0.1}CoO_3$, (b) $LaCoO_3$ (c) $La_{0.9}Ce_{0.1}FeO_3$, (d) $LaFeO_3$; Ce: CeO_2 phase. The other peaks are all due to perovskite phase.

TPD of Oxygen

Figure 4 shows TPD of oxygen from $La_{1-x}Sr_xFeO_3$ (x = 0–0.6), where the rate of desorption calculated from the oxygen concentration in the eluant gas is plotted against the catalyst temperature. It is obvious from this figure that the rate and the amount of O_2 desorption increased with increase in the Sr^{2+} content. For x = 0.2, oxygen desorbed below 800°C amounted to 0.77 ml · g^{-1}, which corresponded to 0.6 surface monolayer of oxygen. The density of oxygen in the monolayer was assumed to

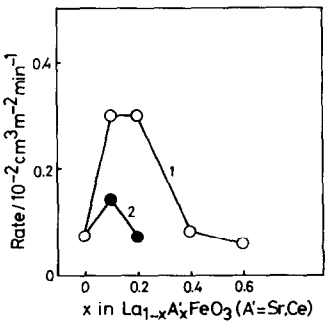

FIG. 2. Effect of Sr^{2+} and Ce^{4+} substitution on the catalytic activities of $LaFeO_3$ for oxidation of propane at 227°C (1 $cm^3 \cdot m^{-2} \cdot min^{-1}$ = 0.045 mmol · $m^{-2} \cdot min^{-1}$). (1) Sr^{2+}, (2) Ce^{4+}.

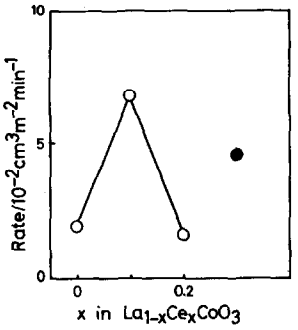

FIG. 3. Effect of Ce^{4+} substitution on the catalytic activities of $LaCoO_3$ for oxidation of propane at 227°C. (●) $La_{0.9}CoO_3$.

be 0.96×10^{15} atom · cm^{-2}. For $x = 0.4$ and 0.6, the amounts of oxygen desorbed up to 500°C corresponded to several layers, indicating that the lattice oxygens in the bulk were desorbed from the samples. The trends observed in the variation with x of oxygen desorption and the similarity of TPD profiles in all $La_{1-x}Sr_xFeO_3$ are very similar to those observed for the Co system (*5*, *6*).

Impregnation of Pt on $La_{1-x}Sr_xCoO_3$ (Pt: 0.1–1 wt%) did not change much the TPD profiles, indicating little promoting effect of Pt for O_2 desorption.

The TPD curves of oxygen from $La_{1-x}Ce_xMeO_3$ (*Me* = Fe,Co) are shown in Fig. 5. The effect of Ce^{4+} substitution was quite different between the Fe and the Co systems. In the case of $La_{1-x}Ce_xCoO_3$, the amounts of desorbed oxygen remarkably

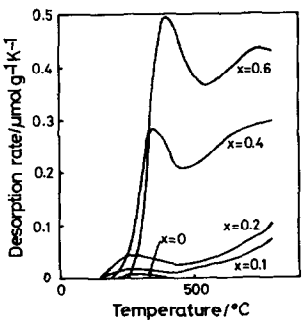

FIG. 4. TPD profiles of oxygen from $La_{1-x}Sr_xFeO_3$ (x = 0–0.6).

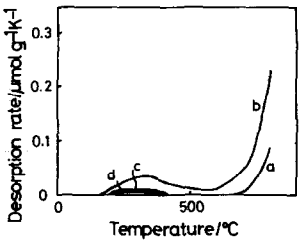

FIG. 5. TPD profiles of oxygen from $La_{1-x}Ce_xMeO_3$ (*Me* = Co,Fe). (a) $LaCoO_3$, (b) $La_{0.9}Ce_{0.1}CoO_3$, (c) $LaFeO_3$, (d) $La_{0.9}Ce_{0.1}FeO_3$.

increased with increase in x and the desorption peaks which appeared at about 300°C were similar to $La_{1-x}Sr_xCoO_3$. On the contrary, in $La_{1-x}Ce_xFeO_3$, the oxygen desorption decreased distinctly by the Ce substitution.

Isotopic Equilibration and Exchange of Oxygen

Results of isotopic equilibration and exchange over $La_{1-x}Sr_xFeO_3$ (x = 0–0.6) are shown in Fig. 6. The isotopic equilibration in the gas phase over $La_{0.8}Sr_{0.2}FeO_3$ proceeded much more rapidly than that over $LaFeO_3$. The isotopic exchange between lattice oxygen and gaseous oxygen over $La_{0.8}Sr_{0.2}CoO_3$ proceeded rapidly, as well. When the oxygens exchanged are ex-

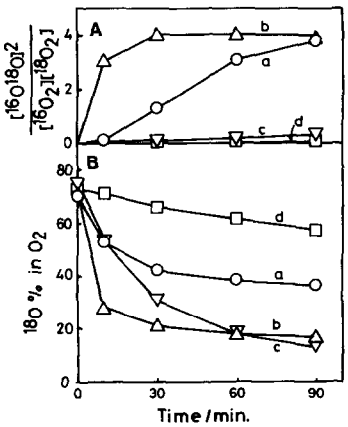

FIG. 6. Isotopic exchange of oxygen over $La_{1-x}Sr_xFeO_3$ at 300°C. (A) Equilibration in the gas phase. (B) Exchange between gaseous and lattice oxygen. (a) $x = 0$, (b) 0.2, (c) 0.4, (d) 0.6.

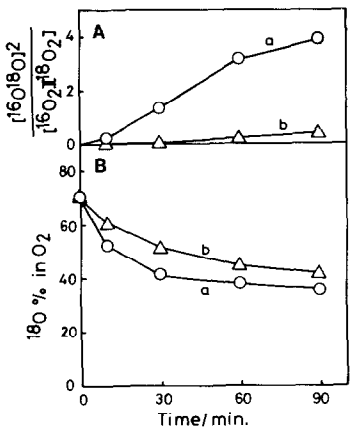

FIG. 7. Isotopic exchange of oxygen over $La_{1-x}Ce_xFeO_3$ at 300°C. (A) Equilibration in the gas phase. (B) Exchange between gaseous and lattice oxygen. (a) $LaFeO_3$, (b) $La_{0.9}Ce_{0.1}FeO_3$.

pressed in the surface oxide layers in which ^{18}O concentration is hypothetically equal to that in the gas phase, the extent of exchange after 90 min was about 2–3 and 11 layers for $x = 0$ and 0.2, respectively. These values were almost the same as those for the $La_{1-x}Sr_xCoO_3$ system (*5*). In contrast, the isotopic equilibration proceeded very slowly both for $x = 0.4$ and 0.6. It was confirmed that these results were reproducible. This trend observed for higher values of x was different from that found for the Co system.

Results of isotope experiments on $La_{1-x}Ce_xMeO_3$ (*Me* = Fe,Co) are shown in Figs. 7 and 8. Both the equilibration and the exchange over $La_{0.9}Ce_{0.1}FeO_3$ proceeded more slowly than over $LaFeO_3$. In the Co system, the exchange rate significantly increased with increasing x, while the equilibration proceeded almost the same over all samples.

DISCUSSION

Structure and Nonstoichiometry

$La_{1-x}Sr_xFeO_3$ forms perovskite structure in the whole range of x ($0 \leqq x \leqq 1.0$) (*8*). According to the literature, $La_{1-x}Sr_xFeO_3$ has the following structures: orthorhombic perovskite ($0 \leqq x \leqq 0.2$), rhombohedral ($0.3 \leqq x \leqq 0.5$), and cubic ($0.6 \leqq x \leqq 1.0$). When Sr^{2+} is partly substituted for La^{3+} in $LaFeO_3$, the oxidation state of Fe changes from trivalent to tetravalent (*9*). With increasing x, a part of the charge compensation is accomplished by the formation of oxygen vacancies ($La_{1-x}Sr_xFeO_{3-\delta}$) besides the Fe^{4+} formation.

$$La^{3+}_{1-x}Sr^{2+}_xFe^{3+}_{1-x}Fe^{4+}_xO_3 \rightarrow La^{3+}_{1-x}Sr^{2+}_xFe^{3+}_{1-x+2\delta}Fe^{4+}_{x-2\delta}O_{3-\delta} + \delta/2O_2$$

For example, it was reported that the value of δ in $La_{0.2}Sr_{0.8}FeO_{3-\delta}$ was about 0.1 in oxygen atmosphere (*8*). The value of δ in $SrFeO_{3-\delta}$ was 0.02 when annealed under 65 atm of oxygen at 1000°C for 24 h (*10*), and *in vacuo* at 1300°C brownmillerite-type structure of $SrFeO_{2.5}$ was formed (*9*). This nature of $La_{1-x}Sr_xFeO_3$ is similar to that of the $La_{1-x}Sr_xCoO_3$ system (*11*).

Though the samples used in the present investigation were polycrystalline powders and were calcined at a relatively low temperature (850°C), the samples had the single perovskite structure in the range $0 \leqq x \leqq 0.2$. The value of δ in these samples may be close to zero, since in the case of the Co system, the nonstoichiometry of powder samples calcined at 850°C was similar to that of single-crystal samples obtained by

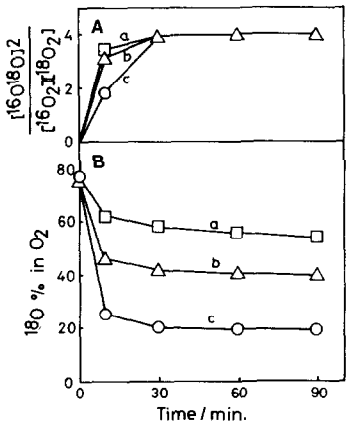

FIG. 8. Isotopic exchange of oxygen over $La_{1-x}Ce_xCoO_3$ at 300°C. (A) Equilibration in the gas phase. (B) Exchange between gaseous and lattice oxygen. (a) $x = 0$, (b) 0.1, (c) 0.2.

high-temperature calcination (*6*). Similarly, the samples probably have the anion-defect structure in the range $x \geqq 0.4$.

All of the Ce^{4+}-substituted samples prepared in the present work contained both perovskite phase and CeO_2 phase, and therefore the substitution ratio of Ce^{4+} in the perovskite phase was not known. However, in $La_{0.9}Ce_{0.1}FeO_3$, CeO_2 phase was almost absent in XRD, indicating that most of Ce^{4+} was substituted for the *A* site of La FeO_3. Since neither the phase of La_2O_3 nor oxides of *B*-site ions appeared in XRD, the major components of the Ce^{4+}-substituted samples were likely $La_{1-x}Ce_y\phi_{x-y}MeO_3$ (*Me* = Co,Fe; $1 > x \geqq y \geqq 0$; ϕ = *A*-site cation vacancy). The formation of *A*-site cation vacancies will be discussed below in more detail.

Effect of Sr^{2+} Substitution on Reactivities of Oxygen of $LaFeO_3$

When Sr^{2+} is partly substituted for the *A* site of $LaFeO_3$, unstable Fe^{4+} is formed in the crystal and the chemical potential of lattice oxygen increases, as in the Co system (*5, 6*). So, the oxygen tends to desorb more easily with increase in the Sr content. Oxygen desorption leaves oxygen vacancy in the lattice, and Fe^{4+} is reduced back to Fe^{3+}. The change of nonstoichiometry in $La_{1-x}Sr_xFeO_{3-\delta}$ with Sr substitution (x), temperature, and oxygen pressure has recently been reported by Mizusaki *et al.* (*12*). According to them, oxygen desorbs in the first step by the change of Fe^{4+} to Fe^{3+}, and in the next stage oxygen desorption takes place by the reduction of Fe^{3+} to Fe^{2+}. The increase of δ or oxygen desorption tended to occur more easily with increasing x.

Therefore, the low-temperature peaks in TPD at 200–500°C observed in the present work presumably result from the reduction of Fe^{4+} to Fe^{3+}. A similar assignment was recently suggested also by Seiyama *et al.* (*13*). This trend explains the increase of oxygen desorption in TPD with increasing x (Fig. 4). The isotopic exchange of oxygen with x ($0 \leqq x \leqq 0.2$) became faster probably by the same reason, since the increase of oxygen vacancies will accelerate both the dissociation of oxygen molecule on the surface by increasing the number of coordinately unsaturated *B*-ion on the surface and the diffusion of oxide ion in the lattice by increasing the number of anion vacancy.

In the range $x \geqq 0.4$, the facility of oxygen desorption in TPD increased remarkably with x. The amount is so great that most of this oxygen is certainly from the bulk. However, the rate of isotopic exchange did not increase and in some case decreased. The decrease appears to be related to the decrease in the equilibration rate. Dissociation of oxygen molecule probably limited the exchange rate to some extent. Parallelism between TPD, equilibration and exchange existed in the case of $La_{1-x}Sr_xCoO_3$ (*5, 6*), but in the Fe system, equilibration at least behaved differently. The reason for the slow dissociation of oxygen molecule is not clear, but the presence of the $SrFeO_{3-\delta}$ phase or some other structural or valence changes at high x values may be responsible. Very slow equilibration and significant exchange found for x = 0.4 and 0.6 may be due to the relative rate of dissociation and bulk diffusion. If the latter is rapid as compared with the former, ^{18}O on the surface is extensively diluted by ^{16}O in the bulk and $^{16}O_2$ would appear in the gas phase. But another possibility as suggested for Cu-zeolite (*14*) cannot be excluded. This behavior is not similar to the Co system

Sr^{2+}-Substitution Effect on Catalytic Activity of $LaFeO_3$

In the range $0 \leqq x \leqq 0.2$ of $La_{1-x}Sr_xFeO_3$, the increase of the catalytic activity for propane oxidation with increase of x may be explained as discussed in the previous papers (*5, 6*); the reactivity or the chemical potential of lattice oxygen increased with the increase of x in the $LaCoO_3$ system. Whether the oxygen directly involved in

the catalysis is the lattice oxygen or adsorbed oxygen is not obvious. Nevertheless, as discussed previously (*6*), it can be at least stated that the oxygen species closely reflects the nature of lattice oxygen, even if it is the adsorbed oxygen. The reason why the catalytic activity decreased significantly in the range $x \geqq 0.4$ may be explained either by the decrease of the reoxidation rate of the sample as in the case of the Co system (*6*), or by the drop of the capability of dissociation of oxygen on the surface with increase of Sr^{2+} substitution, as indicated by the rate of isotopic equilibration (Fig. 6).

Effect of Ce^{4+} Substitution

As described above, the compositions of the catalysts containing Ce^{4+} may be $La_{1-x}Ce_y\phi_{x-y}MeO_3$ with the *A*-site cation vacancies. In $La_{0.9}Ce_{0.1}FeO_3$, Ce^{4+}-substitution ratio (y) is close to x (= 0.1), because the peaks of CeO_2 phase was hardly detected in XRD. In this case, as Ce^{4+} is introduced, a part of trivalent Fe in the *B*-site becomes divalent and makes the oxygen vacancy difficult to be formed, since oxygen desorption at low temperature is due to $Fe^{4+} \rightarrow Fe^{3+}$. Therefore, the facilitation of oxygen desorption in TPD and the rate of isotopic exchange of oxygen decreased with increase in Ce^{4+} content as shown in Figs. 5 and 7. The catalytic activity for propane oxidation increased to some extent with Ce^{4+} substitution (Fig. 3). A possible reason might be that Fe^{2+} ions formed are more catalytically active.

On the other hand, Ce^{4+}-substitution ratio (y) in the Co system may be considerably less than x, as the peaks of CeO_2 phase distinctly appeared in XRD. In this case, the formation of an *A*-site vacancy (ϕ) becomes significant and a part of trivalent Co ion in the *B* site changes to the tetravalent state. Therefore, the effect of Ce^{4+} substitution in the $LaCoO_3$ system is expected to be similar to the effect of Sr^{2+} substitution. This is supported by the increase of the catalytic activity (Fig. 3), the facilitation of oxygen desorption by TPD (Fig. 5, curves 1 and 2), and isotope experiments (Fig. 8). Decrease of the catalytic activity at $x = 0.2$ may be caused by the same reason as in the $La_{1-x}Sr_xCoO_3$ system (*6*) or by the presence of inactive CeO_2 on the surface. Slightly lower rate of equilibration for $x = 0.2$ might be due to the rapid bulk diffusion which dilutes the ^{18}O concentration of the surface.

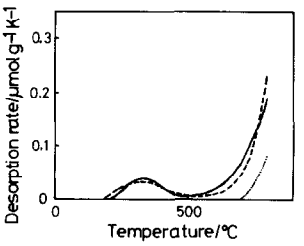

FIG. 9. TPD profiles of oxygen from $La_{0.9}CoO_3$ (solid line), $La_{0.9}Ce_{0.1}CoO_3$ (broken line), and $LaCoO_3$ (dotted line).

To confirm the effect of an *A*-site vacancy, samples were prepared from the nonstoichiometric mixture of La and Co salts (9/10 atomic ratio) which showed XRD peaks derived from only perovskite-type structure, and was supposed to have the composition of $La_{0.9}\phi_{0.1}CoO_3$. TPD of oxygen (Fig. 9) and isotopic equilibration of oxygen on this sample were similar to those of $La_{0.9}Ce_{0.1}CoO_3$, although ^{18}O exchange between gas phase and the bulk was not accelerated. Its oxidation activity for propane was also higher than that of $LaCoO_3$, as expected (Fig. 3).

Thus, the behavior of $La_{1-x}Ce_xCoO_3$ observed in the present work was the same as that of $La_{1-x}\phi_xCoO_3$, except for the difference in the isotopic exchange. Therefore, it is very likely that only a small portion of Ce^{4+} is actually introduced to an *A* site of $LaCoO_3$ and most of the *A* sites which are expected to be occupied by Ce^{4+} form cation vacancies (ϕ).

REFERENCES

1. Voorhoeve, R. J. H., "Advanced Materials in Catalysis," p. 129. Academic Press, New York, 1977.

2. Libby, W. F., *Science* **171,** 499 (1971).
3. Voorhoeve, R. J. H., Remeika, J. P., Freeland, P. E., and Mattias, B. T., *Science* **177,** 353 (1972).
4. Nakamura, T., Misono, M., Uchijima, T., and Yoneda, Y., *Nippon Kagaku Kaishi,* 1679 (1980).
5. Nakamura, T., Misono, M., and Yoneda, Y., *Bull. Chem. Soc. Jpn.* **55,** 394 (1982).
6. Nakamura, T., Misono, M., and Yoneda, Y., *J. Catal.* **83,** 151 (1983); *Chem. Lett.,* 1589 (1981).
7. Shin, S., *Mater. Res. Bull.* **16,** 299 (1981).
8. Gallagher, P. K., and MacChesney, J. B., *Symp. Faraday Soc.* **1,** 40 (1967).
9. Watanabe, H., *J. Phys. Soc. Jpn.* **12,** 515 (1957).
10. Shimony, U., and Knudsen, J. M., *Phys. Rev.* **114,** 361 (1966).
11. Wedsley, A. D., "Non-Stoichiometric Compounds," p. 134. Academic Press, New York, 1964.
12. Mizusaki, J., Yamauchi, S., Fueki, K., Ishikawa, M., and Yoshihiro, M., *Annu. Rep. Eng. Res. Inst., Fac. Eng. Univ. Tokyo* **42,** 155 (1983).
13. Teraoka, Y., Yoshimatsu, N., Yamazoc, N., and Seiyama, T., *Shokubai* **26,** 107 (1984).
14. Iwamoto, M., Morita, S., and Kagawa, S., *J. Chem. Soc. Chem. Commun.,* 842 (1980).